JOURNAL OF BACTERIOLOGY, June 1977, p. 1364-1381

Vol. 130, No. 3
Printed in U.S.A.

Effect of Ethylenediaminetetraacetate upon the Surface of *Escherichia coli*

MANFRED E. BAYER* AND LORETTA LEIVE

The Institute for Cancer Research, The Fox Chase Cancer Center, Philadelphia, Pennsylvania 19111, and the Laboratory of Biochemical Pharmacology, National Institute of Arthritis, Metabolism and Digestive Diseases, Bethesda, Maryland 20014*

Received for publication 18 March 1977

The effect of ethylenediaminetetraacetate (EDTA) on the envelope of two strains of *Escherichia coli* (B and Cla) was studied with freeze-fracturing methods. Untreated cells showed the outer membrane's outer surface with a fine texture of randomly spaced depressions of about 4.5-nm diameter; small areas with symmetrical arrangements of structural surface elements were also observed. The outer membrane's fracture plane revealed a random distribution of particles on its "concave" plane, only occasionally interrupted by particle-free areas. The "convex" aspect of the outer membrane's fracture plane showed only a few scattered particles. The cleavage plane of the inner membrane was often interrupted by many localized elevated plateaus, at which the cleaving process had, for short distances, switched to the outer membrane. The effects of EDTA treatment were mainly seen in the structure of the freeze-etched outer membrane: (i) the pits as well as the symmetrical surface elements of the outer membrane's outer surface had disappeared; (ii) a number of plateaus (about 20 to 50/cell) were seen at which a cleavage plane within the inner membrane had switched to the hydrophobic portion of the outer membrane (outer membrane's fracture plane). These plateaus were also visible in untreated cells; however, EDTA treatment apparently caused an increased exposure of plateaus. Surface areas, exposed by freeze-etching, revealed the underlying plateaus as elevations in the surface contour of the cell, suggesting a slower etching rate in the zones of the plateaus relative to the rest of the outer membrane. Well-defined, particle-free patches in the outer membrane's fracture plane, concave, were more frequent and larger in size after EDTA treatment than in the controls. In the presence of glycerol, the cells often cleaved in the outer membrane's fracture plane, but isolated plateaus were rarely observed. After metabolic poisoning of cells for 15 to 25 min at 37°C, the plateaus had widened. These data suggest that the material of the plateaus has a slow rate of lateral diffusion. Placement of EDTA-treated cells in fresh medium at 37°C caused, after 3 to 5 min, the reoccurrence of the pitted surface structure. We propose that the plateaus represent localized zones, at which newly synthesized lipopolysaccharide has been inserted.

Coliform bacteria, exposed to ethylenediaminetetraacetic acid (EDTA), may lose between a third and a half of their lipopolysaccharide (LPS) and also some smaller amounts of protein and phospholipids (23); such cells become permeable to a variety of metabolites and develop sensitivity to drugs that are normally excluded (21-24, 31). These changes appear to be selective for the outer membrane, whereas many other metabolic functions remain intact (23). The outer membrane, which contains 15 to 40% (by weight) LPS, loses 5 to 20% of its mass after EDTA treatment; however, electron micrographs of conventional thin sections of EDTA-treated bacteria have failed to reveal visible changes in the normal bilayer structure of the outer membrane (8). Since the LPS is the component affected most by EDTA, and since most of the mass of the LPS resides in the polysaccharide portion, which provides only low electron contrast in ultrathin sections, we looked for structural changes in the outer membrane with the freeze-etch technique. This method reveals large surface areas of the envelope and may disclose subtle differences in membrane composition (3-6, 17, 18-20, 34). The method allows observation of number and distribution of intramembraneous particles and

their response to various changes in membrane composition or environment, as has been described for Mg starvation (11, 14), treatment by membrane-directed drugs (13), or lipid phase transitions (4, 37).

Our experiments indicate that EDTA treatment changes the outer membrane and uncovers localized structural domains maintained in a growing cell. These domains are apparently more resistant to EDTA treatment than the rest of the outer membrane. In metabolically inhibited cells, the domains appear to mix slowly with the neighboring EDTA-sensitive areas.

MATERIALS AND METHODS

Bacterial strains, growth conditions, and EDTA treatment. *Escherichia coli* strains B and Cla were grown on nutrient medium (0.5% yeast extract, 1% tryptone, 0.5% NaCl, and 0.1% glucose adjusted to pH 7 with 1 N NaOH) with aeration at 37°C, and were harvested in midexponential growth phase; in another group of experiments, the cells were metabolically poisoned by the addition of deoxyglucose (DOG) (10^{-5} M) and potassium cyanide (KCN) (10^{-3} M) (both Fischer) and maintained for different lengths of time at 37°C before they were subjected to treatment with EDTA. For this, to the cells was added $CaCl_2$ for 5 min to make a final concentration of 50 mM. The cells were then sedimented at 4°C for either 5 or 10 min at 6,000 × *g* and, unless otherwise indicated, suspended in one-tenth the original volume of tris(hydroxymethyl)aminomethane (Tris)-hydrochloride, 0.12 M, pH 8.0. The temperature was brought to 37°C, EDTA (15 mM final concentration) was added, and the cells were incubated for between 3 and 5 min. $CaCl_2$, 40 mM, was added to stop the reaction, and the cells were again sedimented. Cells were also processed either without adding EDTA, or without the addition of $CaCl_2$. In other experiments, the EDTA-treated cells were suspended in fresh nutrient medium and incubated at either 4 or 37°C for various lengths of time.

Assay for release of LPS. EDTA-treated cells from a 200-ml shaking culture and control cells not exposed to EDTA were collected by centrifugation, and the LPS was extracted and purified by the aqueous butanol method (26). The amount of purified LPS was estimated by the phenol-sulfuric acid assay (9) or, occasionally, by estimation of 2-keto-3-deoxyoctulonic acid by the thiobarbituric acid assay (7).

Electron microscopic methods. For freeze-etching, the cells were quickly cooled by dilution in medium of 4°C and centrifuged at 6,000 × *g* for 10 min at 4°C. Additional washings in either cold nutrient medium or in Tris did not seem to affect the fine structure; in most cases, the cells were therefore used without further washing. Glycerol was added to a number of preparations to a final concentration of 15%, and these cells were centrifuged subsequently at 6,000 × *g* for 15 min at 4°C. Small portions of the sediments were quickly transferred to gold support grids and frozen in Freon 12 at the temperature of liquid nitrogen. Freeze-etching was carried out in the Balzer BA 360 M unit, with etching times of 1 to 3 min at −100°C and platinum-carbon shadowing. A modified method was often used for increasing the areas of fractured membrane (see below). The method involves an advanced knife setting of several micrometers before the last (deep) hit with relatively high speed. The replicas were cleaned in 70% sulfuric acid, followed by sodium hypochlorite (4 to 6% solution), and mounted on 400-mesh copper grids. Micrographs were taken at magnifications of 4 × 10^4 in a Siemens Elmiskop 101 electron microscope on Ilford Contrasty Lantern plates.

Stereo tilt angles were kept within ± 5°. The final prints were made from contact copies of the negatives, so that the platinum source of the vacuum evaporator appears as source of illumination and the metal shadows appear dark. Diffractograms were taken on 35-mm film (Kodak plus X) from positive transparencies of the electron micrographs, with a helium-neon continuous-gas laser as light source.

RESULTS

Release of LPS. *E. coli* B and Cla were chosen because they lack surface structures such as type I pili under the growth conditions of our experiments; also, capsular antigens are absent; thus, the cell surfaces are not obstructed by these structures. The cells of both strains released 20 to 30% of their LPS when submitted to the previously described method (21, 22) of EDTA treatment; even much higher EDTA concentrations did not increase the yield of LPS, nor did it result in significant ultrastructural changes in the freeze-etched replicas. However, such refractory strains release increased amounts of LPS, if incubated with Ca^{2+} or Mg^{2+} at relatively high concentrations prior to EDTA treatment (23); after preincubation of the cells in 50 mM $CaCl_2$, subsequent exposure to EDTA released 50 to 55% of the LPS from both cell strains, whereas much less protein and lipids (both below 10%) were extracted (24). Since the cells were not washed after exposure to $CaCl_2$, the EDTA concentration was kept high to chelate the Ca^{2+} remaining in the cell sediments.

Appearance of the cell surface after freeze-etching. For easy identification, we have included a diagram (see Fig. 12) representing the layers of the EDTA-treated envelope and their structural "markers." In the diagram, the outer membrane (OM) is subdivided into the outer face of the OM (OMO) and the fracture plane of the OM (OMF), which exhibits a "convex" face when looking from outside the cell on the remaining fracture plane; looking from inside the cell outward, one will see the corresponding

"concave" face of the OMF. The innermost (concave) plane of the OM, which faces the protoplasmic membrane or the periplasmic space, is the OMI. The position of the peptidoglycan layer remains unknown. This structure may be embedded in the membrane between the OMF and OMI, or it may represent the face OMI. Analogous to the OM, the inner membrane (IM) presents the same number of faces: its outer face (IMO) (however, this face has not yet been made visible unambiguously in complete cells); the inner membrane's fracture plane (IMF), with its "convex" and "concave" aspects; and the innermost face of the membrane (IMI). However, this face, analogous to the OMI, has not yet been demonstrated over larger areas of the membrane. We are presenting micrographs of *E. coli* B only; almost identical results were obtained with the envelope of *E. coli* Cla cells.

Untreated cells: freeze-etching. In freeze-etched replicas, the OMO of unfixed *E. coli* B and Cla was often slightly wavy. At areas of low shadowing angle, a characteristic surface pattern became visible (Fig. 1), which was caused by many small depressions, or "pits." Stereomicroscopy revealed that "pits" are true depressions between a network of more or less contiguous ridges providing the rims of the "pits."

The pits were closely arranged in an apparently nonsymmetrical, random fashion. To determine whether there might be any regularity in their packing arrangement, the pitted area shown in the center of Fig. 1 was used for light diffraction; the method would reveal the presence of repeat structures, or "crystallinity," by production of symmetrical high-intensity spots in a characteristic intensity and distance from the undiffracted portion of the beam. The diffractogram is shown in the insert of Fig. 1. The diffraction lines are shaped like open rings, suggesting a random, rather than an ordered, arrangement of the pits. That only two portions of a circle are seen instead of a fully closed ring is due to the one-directional platinum shadowing, in which only those portions of the pits provide electron contrast that are oriented normally to the direction of the metal vapor; the other portions of the more or less circular pits (and their rims) do not contribute to the diffractogram. The randomly oriented pits measured about 4.5 nm in diameter with a (center-to-center) distance of 9 to 10 nm.

We found the surface pattern more pronounced in *E. coli* B than in strain Cla. Treatment with $CaCl_2$, with or without subsequent exposure to Tris-hydrochloride, had no structural effect. Prolonged etching times (up to 6 min at −100°C) as well as brief washing of the cells in synthetic medium (TPG3A) (32) or F-medium (1) increased the depth of the pits. At relatively limited areas we observed, in addition, a regular surface pattern (Fig. 2) produced by the symmetrical distribution of well-separated, knoblike protrusions or stubs, measuring 5 to 6 nm in diameter with a center-to-center distance of 7 to 8 nm. The symmetry of their arrangement is also depicted by the diffractogram (insert, Fig. 2), for which the central third of the area shown in Fig. 2 was used as a diffracting object. One observes two pairs of spots in a distance corresponding to 7 and 8 nm on the cell surface. Another pair of spots, which one might expect if a sixfold arrangement of the protruding elements existed, might possibly become "shaded" due to the one-directional shadow-casting method employed. In the zones at which areas of symmetrical and random arrangement were joining, the transition from one pattern to the other was smooth, with no apparent structural disturbances or mismatches. We assume that in the noncrystalline zones, the protruding elements are interconnected with their neighboring protrusions, thus forming the rims of the pits, so that the same surface elements may be arranged in the two different ways. It appears that the regular arrays cover only smaller portions of the cells of our preparations; however, in some preparations, the regular areas are found frequently enough to assume their presence in possibly more than 50% of the cell population. The conditions by which the regular arrangements may be produced have not been established. Cooling of the cells at various rates did not affect the relative amount of the random and nonrandom surface pattern. None of these surface arrangements can be observed in glycerol-treated cells under conditions of our experiments (Table 1), since their OMO will not be exposed.

Fracture planes of the envelope. A rather narrow fracture was frequently seen in the OM, representing a short exposure of the intramembraneous OMF of the OM. This typical fracture of the *E. coli* OM (6, 27, 28, 39) has been assigned to the hydrophobic region within the OM (17, 20) (white arrows on Fig. 1). In glycerol-treated cells, this OMF is exposed to a much larger extent. We were able also to enhance the areas of this OMF without the use of glycerol by applying the fracturing knife at an experimentally established speed and increasing the knife-advance setting. In the subsequent text, this method shall be called "deep fracturing."

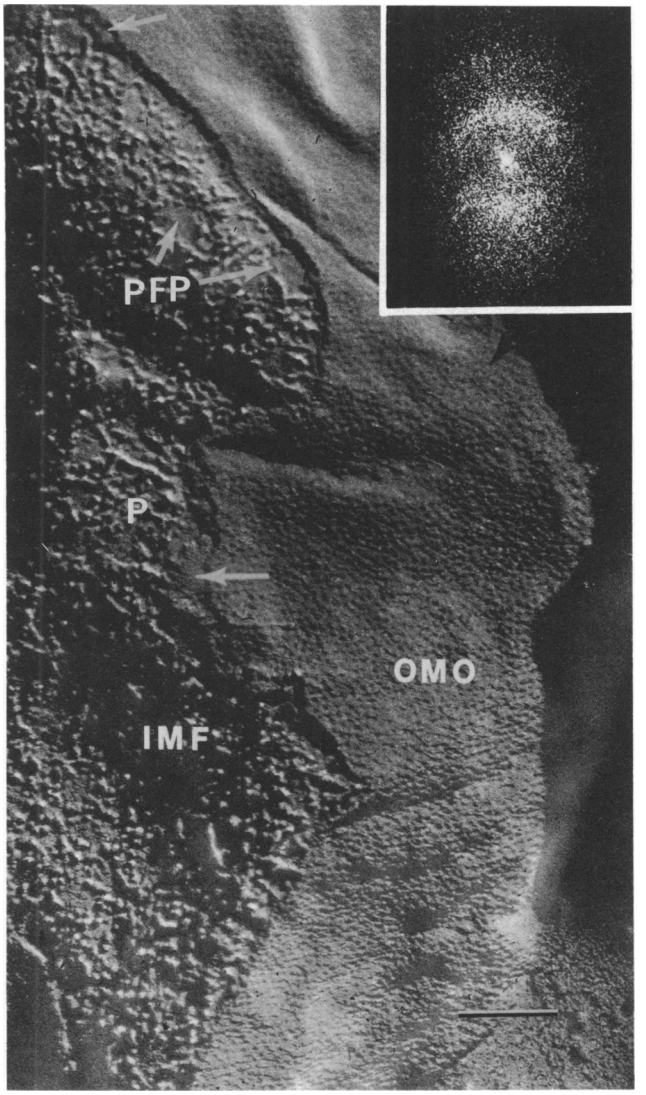

FIG. 1. *The surface of freeze-etched E. coli B. Note the pitted surface, the narrow fracture step in OMF (white arrows) and IMF. Insert shows diffractogram for which the central area of OMO was used. The ring-shaped intensity distribution on diffractogram indicates random distribution of surface pattern (see text). Symbols: OM, outer membrane; IM, inner or plasma membrane, each membrane having an outer (prefix O) and an inner (prefix I) surface. The intramembraneous fracture planes are designated by added F: OMF, IMF. Each of the fractures produces two surfaces, one "convex" and one "concave." White arrows point to narrow fracture areas in OMF; P, particles within fracture plane of IMF; PFP, particle-free patches; X, with arrow, indicates particles that appear on surface of cells (OMF) after EDTA treatment (see text); PL, plateaus protruding from IMF into OMF (see also diagram, Fig. 12). The black arrow indicates the direction of metal evaporation. The bar repesents 0.1 μm.*

With both methods, the convex as well as the concave aspects of the fracture OMF were exposed equally well (see subsequent micrographs and Table 1).

The convex face of the OMF exhibited spherical as well as filamentous particles, about 10-nm diameter, of relatively low density per area, whereas the concave fracture face showed a dense but not complete cover of particles of 5- to 7-nm diameter attached to a much finer granular matrix (see Fig. 10b). It appears that the OMI can be seen only in relatively narrow

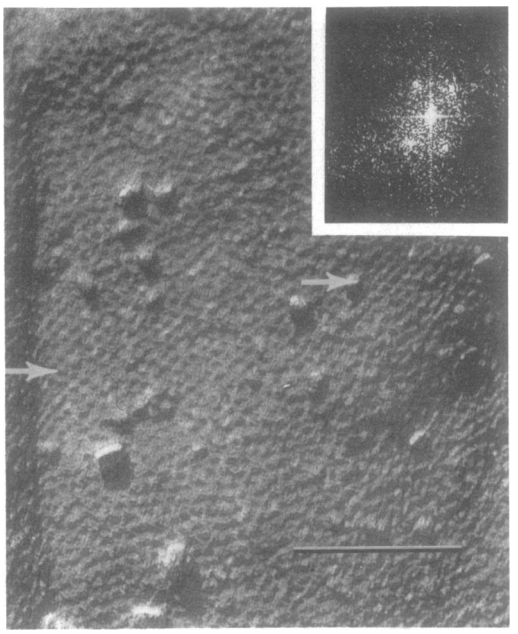

FIG. 2. *Freeze-etching reveals areas of OMO with regularly arranged patterns (see also Fig. 1). The crests between the pits seem to resolve into isolated protrusions or knobs. The few larger spherical particles of irregular distribution are most likely elements readsorbed from the vacuum. The insert is a diffractogram using the regular pattern in the center area of this micrograph as diffracting object. The four high-intensity spots around the center (zero) maximum indicate a repeat structure of ~7.0 and 8.0 nm, respectively, along the two axes.*

areas (see Fig. 5). However, since the exact location of the peptidoglycan layer has not been established, the plane OMI might expose one face of the peptidoglycan layer. Occasionally a few particles measuring 15 to 20 nm in diameter seemed to be associated with this layer.

The fracture through the protoplasmic membrane, or IMF, showed its convex face studded with particles of about 8-nm diameter (Fig. 1, 3, 6–8), whereas the concave face exhibited only relatively few scattered particles (Fig. 4, 5, 9, 10a, 11). This typical distribution of the intramembraneous particles made it possible for us to use this membrane as a marker, for example, after considerable structural changes were introduced in the cell envelope by treatment with EDTA. In glycerol-free preparations of the control cells, we found rather frequently with our cleaving technique small island-like areas at which the IMF had switched to the OM; this generated the aspect of raised plateaus or islands, which were protruding from the level of the IMF (convex) into the OM (Fig. 3). This feature becomes very frequent in EDTA-treated cells and was only on rare occasions demonstrable in glycerol-treated and in sucrose-treated cells (6).

At the expected location of the IMI, protoplasmic surface, larger patches with a smooth surface were often observed as they protruded slightly from the concave IMF into the protoplasmic region (Fig. 4). We have tentatively assigned the surface of these areas to the IMI. Their relative arrangement can best be visualized in the stereo micrographs (Fig. 4; see also diagram Fig. 12).

In addition, the diagram in Fig. 12 shows the IMO; however, we were unable to trace this surface unambiguously, even after use of stereomicroscopy. Whenever it appeared to reveal itself, it was observed in areas that were either folded or in some aspects unusual. Thus, the surface structure of the IMO remains largely unknown and has, therefore, been shown without substructure in the diagram.

Effect of EDTA treatment. Significant ultrastructural changes were observed only in cells pretreated with calcium. It appears that more than 30% of LPS has to be extracted (with some lipids and protein) before unambiguous effects of EDTA treatment can be found. Most structural changes were seen in the OM (Table 1).

(i) The pattern of pits disappeared from the freeze-etched OM, resulting in a smoother cell surface. Large portions of the freeze-etched OM seemed to be thinner than in untreated cells. The smooth areas in Fig. 10 (around the letters OMO, for example) may represent such "thin" zones. Thinning could be caused by an increased speed of etching due to the loss of about 50% LPS after EDTA treatment. Irregularly scattered, more or less spherical particles of approximately 10 nm were often seen (Fig. 9) as they protruded over the level of the cell surface (arrows plus X, Fig. 9).

(ii) A further effect was the appearance of relatively thicker plateau-like localized areas, bulging the cell surface contour, as if at their location the process of thinning had not taken place. Plateaus such as these were not observed in the freeze-etched OMO of untreated cells.

In the freeze fractures through the OM, both the convex as well as the concave aspects were clearly observed. Most striking, however, was the presence of the plateaus, with their bases at the convex IMF; they showed a jagged contour; exposure of intramembraneous particles added to the irregularity of their circumferences. EDTA-treated cells exhibited in their concave OMF the densely packed particles already described for untreated cells; in general, the visibility of these particles seemed less pronounced

TABLE 1. *Layers and cleavage planes of the E. coli envelope as seen after freeze-fracturing and -etching*[a]

Treatment	Layers											
	OMO		OMF		OMI[b]	IMO			IMF		IMI	
	Nutrient medium (glycerol not present) deep fracture method plus etching	Visible in glycerol	Nutrient medium (glycerol not present) deep fracture method	Visible in glycerol	Deep fracture method	Visible in glycerol	Nutrient medium (glycerol not present) deep fracture method plus etching	Visible in glycerol	Nutrient medium (glycerol not present) deep fracture method	Visible in glycerol	Deep fracture method	Visible in glycerol
Convex: No EDTA	Pitted, occasionally "knobbed," in regular symmetrical arrays	Not	Relatively narrow areas exposed, studded with particles, of 8 to 10 nm; some fibers, wide areas visible after "deep-fracture" procedure; particles of 8 to 10 nm; plateaus often visible	Large areas exposed, with particles of 8 to 10 nm	–	–	Not visible	Not identified unambiguously	Abundant (typical) particles of 7- to 10-nm diameter; filamentous particles (pulled out?); particle-free patches (depending on cooling rate)	Yes	–	–
After EDTA	Smooth, with few particles, thinned-out; plateaus bulging cell surface	Not	Many plateaus visible reaching into this layer, some with fibers originating at IMF; in poisoned cells, the plateaus widen after 15 to 25 min at 37°C	Plateaus not visible (with very few exceptions)	–	–	–	–	Plateaus rise from this layer reaching OMF; no obvious change in intramembraneous particles	As above, but no plateaus visible	–	–
Concave: No EDTA	–	–	Background fine grain; 5- to 7-nm particles densely spaced; occasional particle-free areas	Background fine grain; 5- to 7-nm particles densely spaced; occasional particle-free areas	In narrow areas-smooth, perhaps a few particles 10–15 nm in diameter	–	–	–	Large areas exposed; much fewer membrane particles (7 to 10 nm) as on convex plane Localized fractions breaking into OMF concave, representing negative casts of plateaus	Large areas exposed; much fewer membrane particles (7 to 10 nm) as on convex plane Localized fractions breaking into OMF concave, representing negative casts of plateaus	Circular areas with smooth surface protruding from IMF Possibly more of these patches are seen after EDTA	Circular areas with smooth surface protruding from IMF Possibly more of these patches are seen after EDTA
After EDTA	–	–	Increase in particle-free areas	Increase in particle-free areas	Visible after "deep fracture"	Yes	–	–	No additional obvious effect of EDTA	No additional obvious effect of EDTA	–	–

[a] For localization of the planes, see diagram Fig. 12.
[b] This layer might include the peptidoglycan.

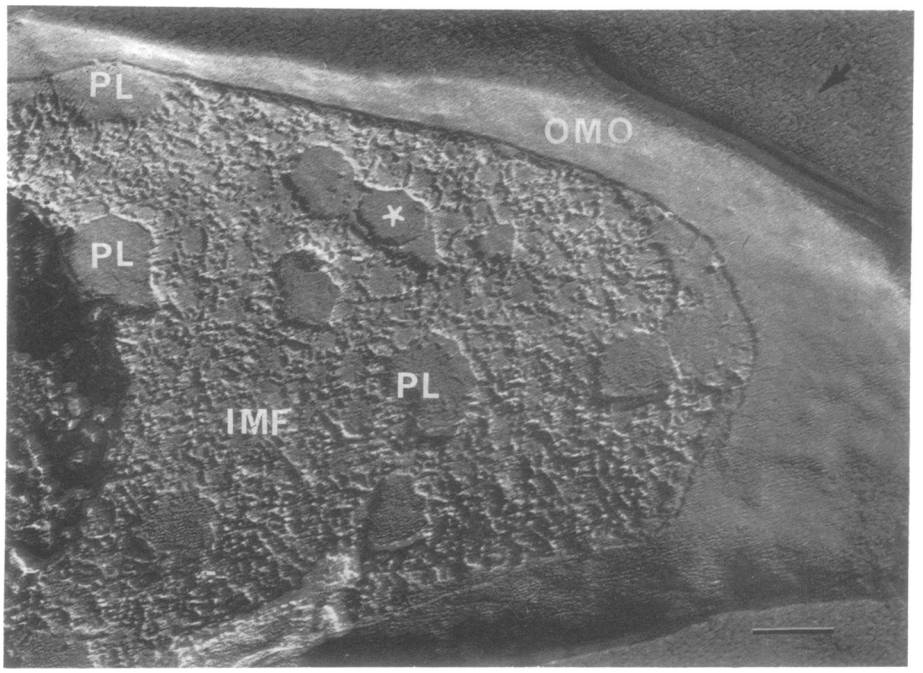

FIG. 3. *In a growing culture as well as after a few minutes with KCN poisoning at 37°C, as shown here, plateaus emerge from the (convex) IMF; the outermost planes of the plateaus reach into the OMF. In very rare instances, a plateau is seen with an additional layer of material on top of it (indicated by a star = OMO). Symbols: See legend Fig. 1.*

than in the untreated control cells. In addition, the particle-free smooth areas were dispersed in this layer (Fig. 10c, black hollow arrows). Compared with the concave fracture face of untreated controls, these particle-free areas appeared to be larger in size and more abundant. Sometimes, however, the treated cells showed an even distribution of particles in this fracture plane (cf. Fig. 10b with c). At the "break-in" areas, the particles of the OMF concave seem mostly to be missing (Fig. 10a). The convex face of this fracture plane did not reveal significant differences between untreated and treated cells.

The fracture faces of the IM showed, at their convex face, the typical intramembraneous particles of 6- to 8-nm diameter in apparently random distribution; we have found no unambiguous sign of a gross redistribution of intramembraneous particles after EDTA treatment. The concave fracture face, with its rather sparse particles, showed occasional zones at which the fracture broke into an underlying plane, most likely representing the concave face of the OMF (Fig. 10a). As mentioned above, the most conspicuous structures originating from the convex fracture plane of the IM were the plateaus reaching into the OM. EDTA treatment enhanced their visibility in the OMF and seemed to increase their frequency compared with the plateaus found in our deep-fracture preparations of untreated controls: after EDTA treatment, plateaus were visible in about 80% of the fractured cells and only in about 20% of the fractured control cells. As in untreated cells, the plateaus in the treated cells probably reach the height, above the IM, of the OMF. This phenomenon is most clearly seen in freeze-etchings such as Fig. 8, which reveals (at the upper fracture line of the envelope) a step between the OMO and the plateau level in an EDTA-treated cell. A similar height is shown by plateaus in untreated cells (Fig. 3).

As stated above, the morphological changes were largely reduced or absent if the cells were not exposed to $CaCl_2$ prior to EDTA treatment. On the other hand, the changes caused by EDTA were not reversed by subsequent addition of $CaCl_2$.

When EDTA-treated cells were diluted into fresh medium and grown for 3 min or more at 37°C, the pitted pattern started to reappear and the cells looked identical to untreated cells (Fig. 13); exposure to fresh medium at 4°C did

not reveal such a change. With the reappearance of the pitted surface, the visibility of the plateaus buckling the OMO vanished. However, in a few cells, they were still visible 8 min after exposure to fresh medium at 37°C.

Spreading of the material composing plateaus. We asked the question whether the plateaus were structures possibly maintained by growth of a cell, or whether they were transient, consisting of material that would eventually mix with those areas which appeared to be more affected by EDTA? To answer this question, the synthesis of cell envelope components was inhibited by addition of KCN-DOG, while the cells were maintained for a given time at 37°C; subsequently, they were rapidly cooled and then either treated with EDTA or left untreated. We found that periods of metabolic poisoning at 37°C for 1 or 5 min caused no significant change in the structural aspect of the control cells (Fig. 3) nor an obvious change in the response to EDTA (Fig. 8). Incubation with metabolic poison for 15 to 25 min at 37°C revealed an increased frequency of extended fractures within the OMF of the control cells (Fig. 6), sometimes fracturing entirely along this plane (Fig. 7). When such cells were EDTA-treated, fewer but larger circular plateaus (Figs. 14a, b) were observed. We interpret this widening of the plateaus as caused by diffu-

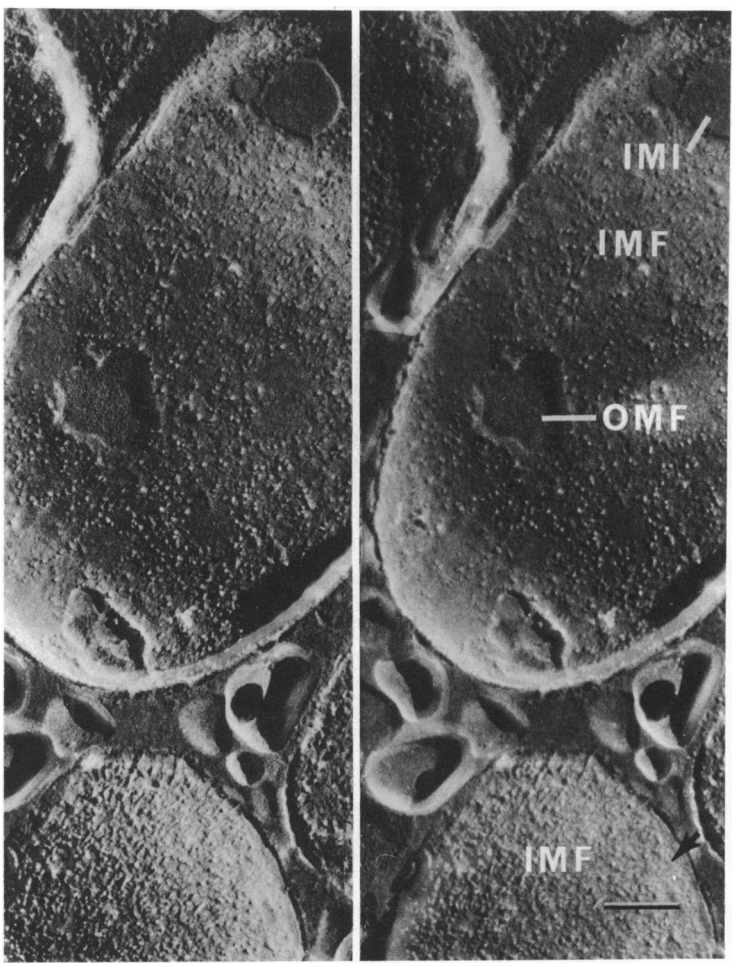

FIG. 4. *Stereo pair of a freeze fracture through the envelopes of two glycerine-treated unpoisoned cells. (i) Upper cell: exposure of the concave face of the IMF. At one area, the IMI seems to be present (patch IMI at upper right portion of the micrograph). At another area, the fracture has broken through the IM plane toward the OM, exposing the concave face of the OMF; (ii) Lower cell: exposure of convex IMF. Symbols: See legend Fig. 1.*

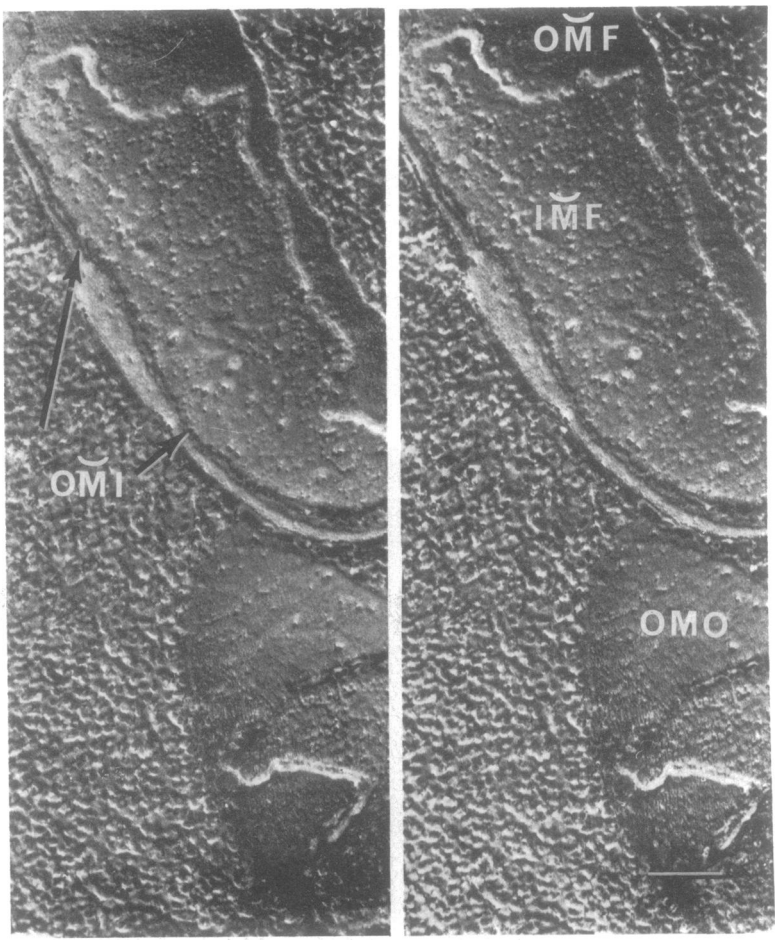

FIG. 5. *Stereo pair of a freeze fracture of unpoisoned, but glycerol-treated cells exposing "concave" and "convex" membrane aspects of their envelopes. (i) Upper cell shows the "concave" IMF with a relatively small number of scattered particles; a narrow step seems to reveal the OMI and, after a further step, the fine granular concave OMF. (ii) Lower cell shows a narrow fracture step in OMF; in a further step the envelope has fractured into the inner membrane, IMF; this plane is studded with numerous intramembraneous particles. Symbols: See legend Fig. 1.*

sion of their components, which eventually results in formation of an uninterrupted fracture plane of the OMF.

If cells were first cooled to 2°C for either 5 or 10 min, and subsequently allowed to grow for 5 min at either room temperature or at 37°C, their OMF was indistinguishable from that of untreated cells. Thus, shorter exposure to low temperatures did not alter the envelope's cleavage pattern.

DISCUSSION

A fine structure of pits or dimples of the OM has been described for a number of bacteria, such as *Neisseria gonorrhoeae* (37); these cells show, in addition, numerous holes of 8.0-nm diameter in their OM. Pits of similar dimensions have been reported for *Klebsiella pneumoniae* (35) and in *Salmonella typhimurium* (34). In the latter report, the pittedness was seen only in rough LPS mutants, whereas this feature seemed to be lacking in smooth strains. Pits of similar dimensions were also described for *Thiobacillus* species (19) and *Acinetobacter* (33).

Our results indicate that EDTA treatment changes the OM of *E. coli* in such a way that freeze-etching depicts areas of relatively high EDTA resistance; in untreated cells, these "prospective" plateau areas are probably repre-

sented by plateaus seen only after freeze cleavage of the envelope. In addition, the EDTA-treated cell loses its characteristic surface pattern of pits. Concomitant with these structural changes, LPS is released, and the envelope permeability is increased by this treatment. Divalent cations, added in the presence or absence of the released material, do not reverse the changes, whereas within a few minutes of exposure to normal medium permitting growth, the surface structure returns to its normal pitted appearance. The pits reappear in about 15 to 20% of a doubling time, followed shortly by the disappearance of the areas showing a thinned OM. The return of the permeability changes to their "normal" values seems to require about half a generation time (16, 21). However, it should be pointed out that a quantitation of these events with microscopic methods such as freeze-etching is difficult: the pittedness will be visible only with optimal shadowing angle and the proper amount of metal evaporated. Furthermore, on a somewhat wavy surface, only a fraction of the visible (perhaps 20 to 50%) etched surface will reveal the fine structure. Therefore, the rate of "recovery" between the morphological and the physiological events may not be too different.

It has previously been demonstrated that EDTA releases half of the OM LPS and little else (possibly 10% of the OM protein and lipid) (24). It is thus reasonable to assume that the observed surface pittedness is linked to the presence of LPS; its loss may be solely due to removal of LPS molecules (28), but it is more likely caused by the disturbance of the entire macromolecular arrangement of the membrane, in which other membrane components (such as proteins) are also involved as linking elements in complexes with LPS (40). EDTA treatment without preincubation with Ca^{2+} results in lowered LPS release accompanied by little or no change in surface structure of these cell strains. The apparent thinning of the OM may reflect the partial loss of LPS affecting the density distribution of the hydrophilic carbohy-

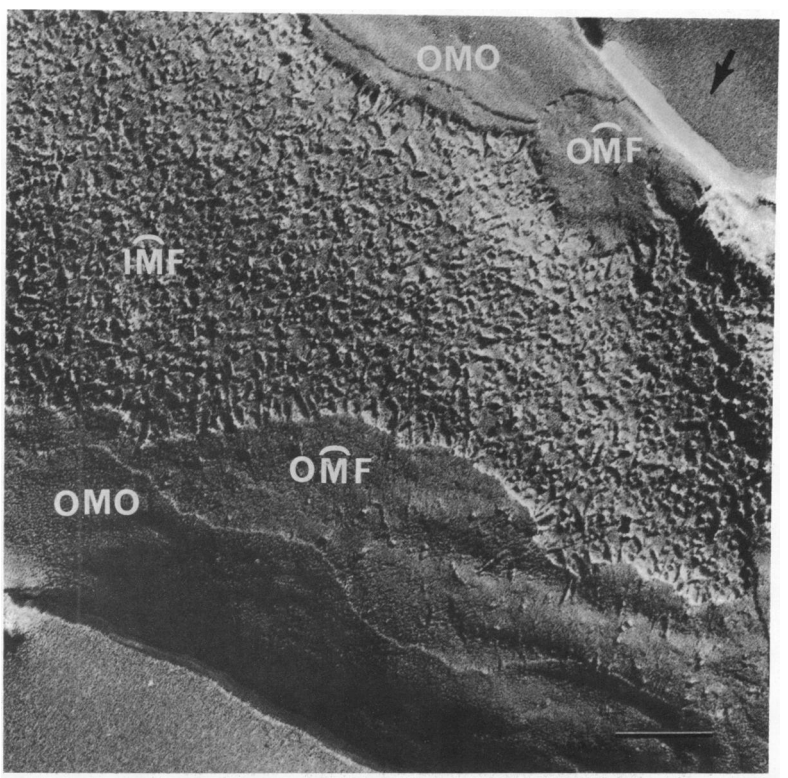

FIG. 6. *A cell, freeze-cleaved with the deep-fracture method, in the absence of glycerol, after KCN-DOG poisoning and prolonged exposure (25 min) to 37°C. Compare to Fig. 3. The single plateaus have disappeared and a uniform layer of OMF becomes visible. Symbols: See legend Fig. 1.*

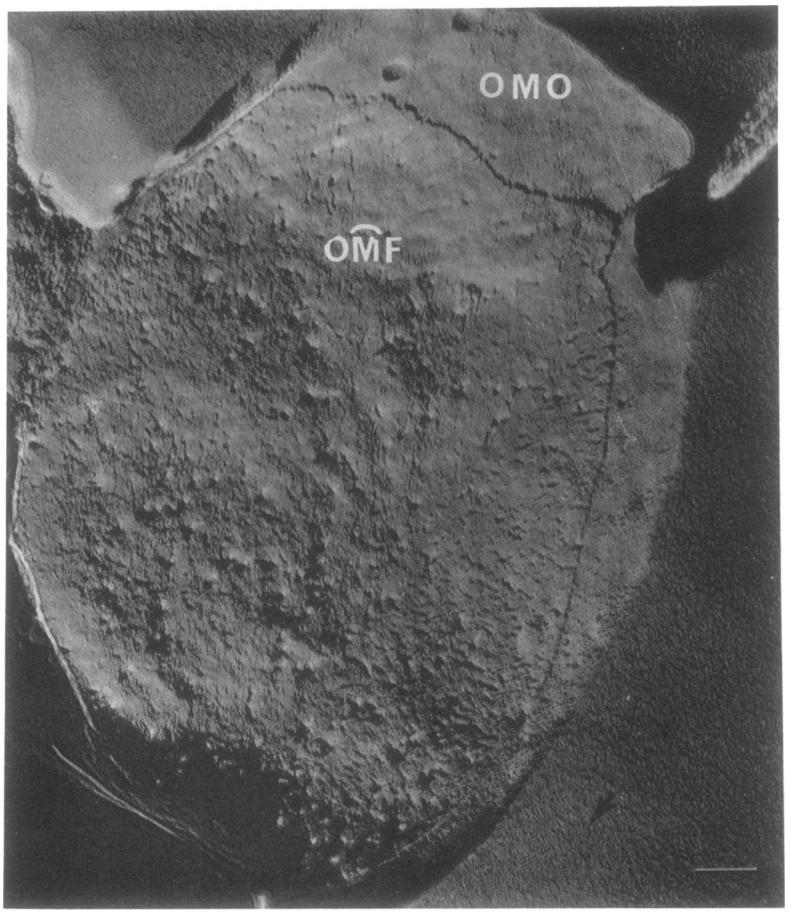

FIG. 7. *After deep fracture in the absence of glycerol, in many cells the prolonged exposure (15 min) to KCN-DOG at 37°C causes the fracture to follow entirely plane OMF. Symbols: See legend Fig. 1.*

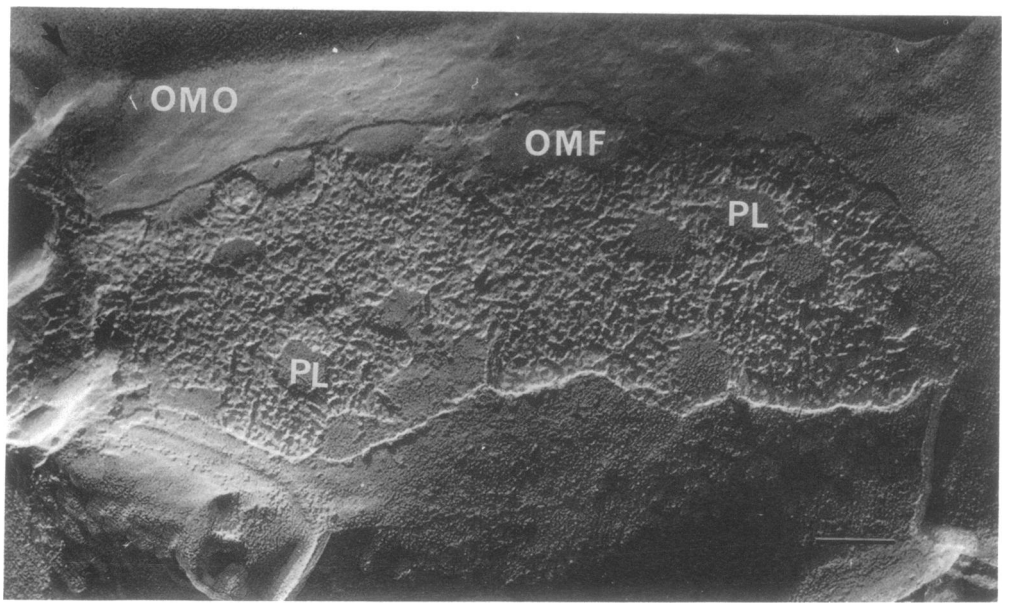

FIG. 8 to 14. *Cells after EDTA treatment.*

FIG. 8. *EDTA treatment exposes the plateaus in the majority of cells. Their relationship with the OMO can be seen in the upper portion of this deep fracture of a cell; by comparing the apparent height of the plateaus with that of the cleavage zone exposing OMF convex, one observes that these levels are of equal height. Symbols: See legend Fig. 1.*

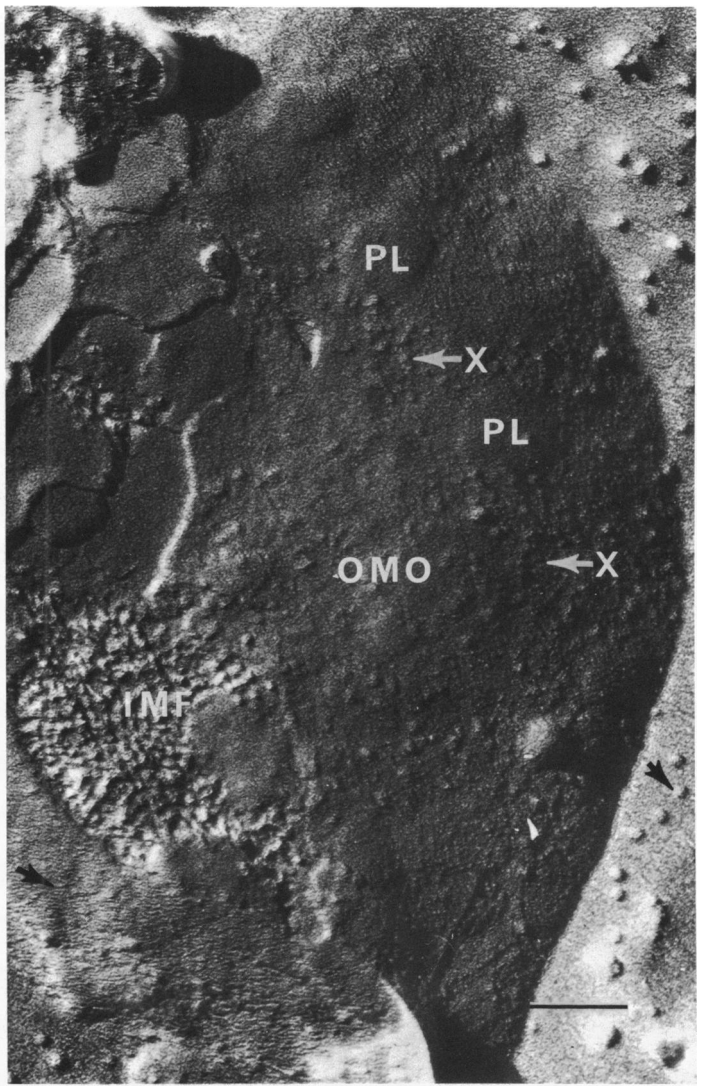

FIG. 9. *OM has changed to a thinner structure so that the plateaus (PL) are bulging the OM surface. Many particles (X) are seen on the surface. Symbols: See legend Fig. 1.*

drate portions, as well as that of the lipid A portion which intercalates the LPS into the lipid bilayer (12, 24). The plateaus are apparently present in the untreated cell, but are not bulging the OM surface. We hypothesize that the increased "porosity" of the treated membrane makes it more susceptible to freeze-etching, due to a relatively increased access of its water to sublimation. The thicker plateaus may thus reflect areas with relatively unchanged or unextracted LPS. Since newly synthesized LPS appears to be nonreleasable in EDTA (25; see also 28), we propose that the plateaus might represent domains of newly synthesized LPS. Their number per cell (between 20 and 40) agrees with the number of LPS insertion sites in *Salmonella anatum* after conversion by phage ϵ15 (3).

The data suggest that after freeze cleavage the surface of a plateau represents the cleavage plane within the hydrophobic portion of the OM (OMF), as shown in Fig. 6. Normal *E. coli* apparently fracture rarely within this plane, whereas EDTA-treated cells do so more frequently. Interestingly, some *E. coli* mutants, in which the protein content of the OM is reduced and the lipid increased, show increased fracturing within this plane (5) as do analogous mutant strains of *Salmonella* (20, 34). Thus, EDTA treatment and mutational reduction of

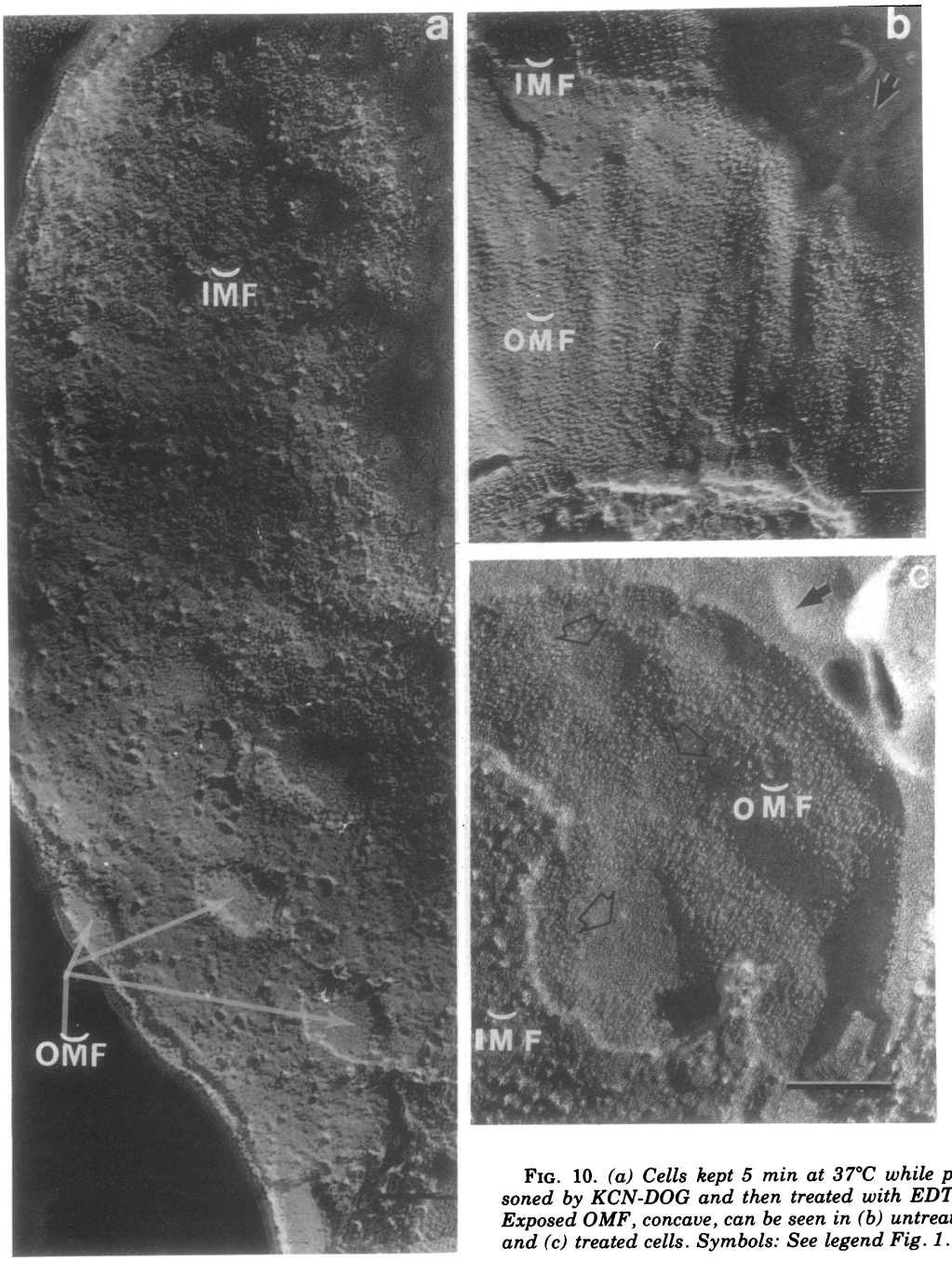

FIG. 10. *(a) Cells kept 5 min at 37°C while poisoned by KCN-DOG and then treated with EDTA. Exposed OMF, concave, can be seen in (b) untreated and (c) treated cells. Symbols: See legend Fig. 1.*

protein may both create OMs with similar physical properties.

The material in the plateaus seems to mix with the thinned portion of the OM at a rate slower than expected for lipid membranes. Experiments with mobilities of spin-labeled fatty acid probes and protein fluorescent probes of biological membranes show rather fast molecular mobilities (17). However, our recent observations suggest that such a movement can be very restricted, as shown by the very slow spreading of LPS in *Salmonella* after conver-

sion by phage (3), and by the finding that the mobility of spin-labeled probes in isolated OMs is also very restricted (S. Rottem and L. Leive, J. Biol. Chem., in press). The latter experiments revealed that the reduced mobility is correlated to qualitative differences in the LPS.

The large "holes" sometimes observed in the concave IMF after EDTA treatment occupy an area and depth that corresponds to that of the plateaus protruding from the convex IMF (Fig. 4). The holes would thus represent the "negative casts" of some of the plateaus; pulling away of the plateaus during cleaving would cause exposure of a matching portion of the concave plane of the OMF.

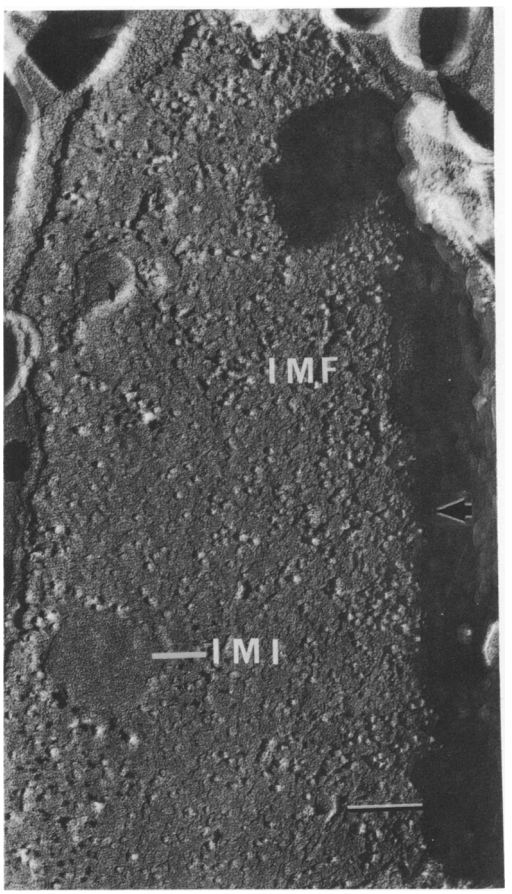

FIG. 11. *IMF concave aspect of an EDTA-treated cell freeze-cleaved in glycerol. At two circular areas slightly elevated plateaus are visible, possibly representing the IMI. The three-dimensional impression is enhanced when the picture is turned 90°, so that the black arrow points from top to bottom. Symbols: See legend Fig. 1.*

It seems important to mention here that the conditions of temperature shift, including those necessary for rapid handling of the specimen before freezing, were kept the same within each group of experiments; this becomes important in the light of the observation of Tsien and Higgins (38) that the distribution of plasma membrane particles of *Streptococcus fecalis* depends on the temperature pretreatment of the cells prior to freezing. Furthermore, the compositional changes of the membrane due to a redistribution of intramembraneous proteins after cooling (4, 18) make a standardized procedure obligatory. Regular alignments of the particles in the IM cleavage plane (IMF), similar to those reported for *E. coli* after extensive Mg^{2+} starvation (11), were not observed.

The morphological effect of EDTA on *Pseudomonas aeruginosa* has been described by Gilleland et al. (14). Obviously, EDTA has a more pleiotrophic effect on this organism than on *E. coli*. The reason for this might be that, in *Pseudomonas*, EDTA causes not only LPS release and permeability changes, but also affects the osmotic stability of the cells and leads to cell death (2, 10, 16, 29). In contrast, *E. coli* B survives quantitatively the EDTA treatment within the time periods of our experiments. Gilleland et al. (15) reported for *Pseudomonas* a change in the concave OMF after EDTA treatment and ascribed the effect to a release of a membrane LPS-protein complex (30), indicating that this layer represented a Tris-EDTA-sensitive site in the cell wall of *P. aeruginosa*. In agreement with this, we have found an increase in numbers and a widening of particle-free areas in the concave OMF of EDTA-treated cells. It is interesting that *Pseudomonas*, after growth in Mg^{2+}-deficient medium, assumed a relative resistancy to subsequent EDTA treatment (14).

Morphologically, the EDTA-resistant cells were reported to show an uninterrupted layer of particles in the concave OMF. This result strengthens the suggestion of Gilleland et al. that EDTA sensitivity is reflected in the extractability of portions of this particulate layer (14). Stinnet and Eagon showed that the structural defect can be repaired after incubation of *Pseudomonas* osmoplasts into fresh medium (36). It is interesting that such incorporation occurs, although the EDTA treatment rendered the cells nonviable. The extent of changes we observed in the corresponding fracture plane of *E. coli* B is much less than that described for *P. aeruginosa*. Whether this fact can be correlated with the observed EDTA stability of the *E. coli* strains remains to be studied. The necessity of

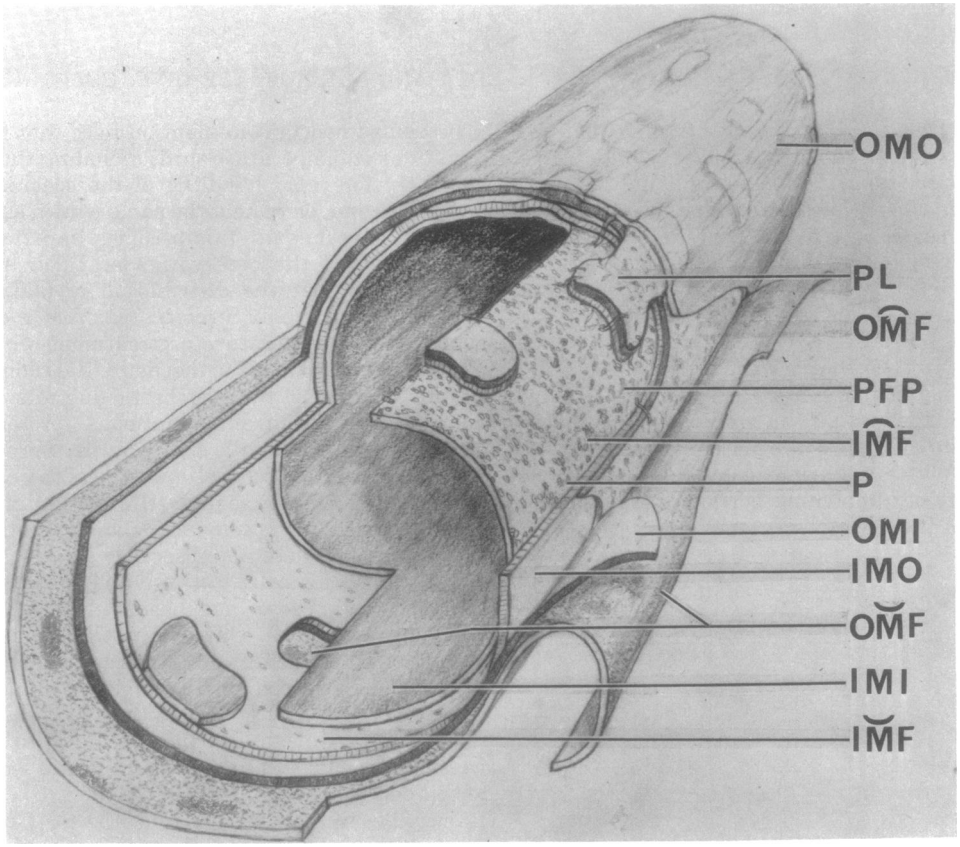

FIG. 12. *Diagrammatic representation of the freeze-etched surfaces and the various fracture planes and faces of the E. coli cell envelope after EDTA treatment. For symbols, see legend Fig. 1. In addition, the symbol ⌣ has been introduced for the concave membrane fracture faces and ⌢ for the convex fracture faces.*

FIG. 13. *Surface of a cell treated with EDTA and subsequently washed and exposed for 3 min to fresh medium at 37°C; the surface pattern of pits has returned. Symbols: See legend Fig. 1.*

osmotic stabilizers ("cryoprotectants") in cell preparations of *Pseudomonas* to be treated with EDTA excludes the possibility to visualize the outermost surfaces of these cells by freeze-etching methods. Cryoprotection also eliminates the visibility of the plateaus. While Mg starvation causes disorganization of the envelope of *Pseudomonas* (14) and a disturbance of

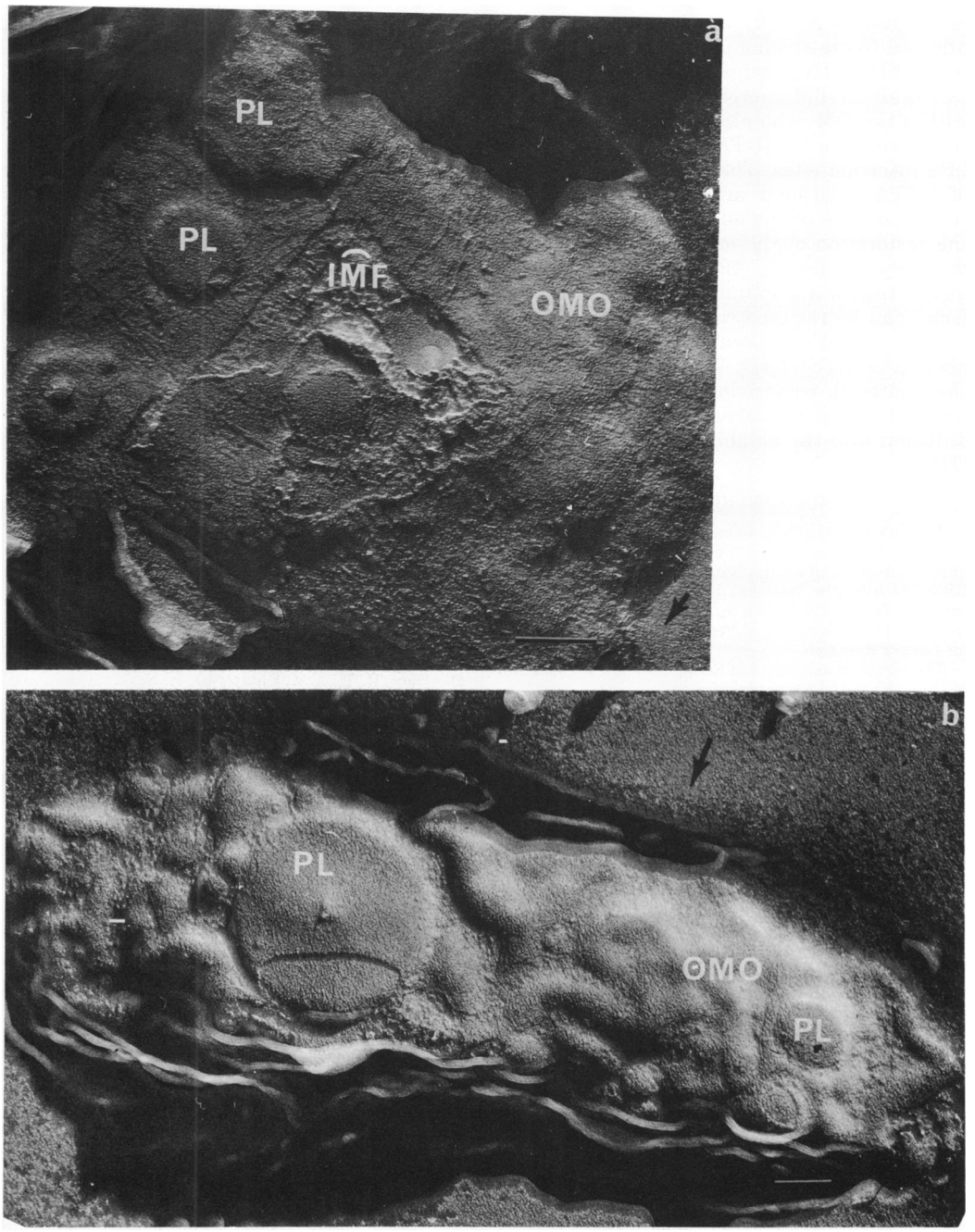

FIG. 14. *(a) Culture poisoned for 15 min at 37°C and subsequently treated with EDTA. The relatively large circular plateaus can be seen as they bulge the OMF. The fracture into IMF depicts a relatively thinned OM. (b) Culture treated exactly as (a); relatively large circular areas are frequently seen. Symbols: See legend Fig. 1.*

the IM of *E. coli* (11), the depletion of Mg^{2+} by EDTA has relatively ill-defined effects on the IM of both species.

In conclusion, we report here that EDTA causes drastic physical changes in the outer membrane of *E. coli*, which are expressed in unusual freeze-etching and freeze-fracture patterns. EDTA treatment seems to enhance subtle localized differences of membrane areas within the OM. The plateaus, with their relative resistance to EDTA, might be related to LPS insertion sites. The morphological effects of EDTA treatment are concomitant with a release of 50% of the envelope LPS. Although the restoration of the original content of LPS probably requires a time span considerably longer than a few minutes, the structural "defects" can be restored rather quickly by exposure to conditions permitting growth in the absence of the chelator. When growth is halted, the material comprising the local plateaus seems to spread relatively slowly by lateral diffusion into the neighboring material of the OM.

ACKNOWLEDGMENTS

This investigation was supported by grant BMS73-01121 from the National Science Foundation to M. E. B. and grants CA-06927 (from the National Cancer Institute) and RR-05539 from the National Institutes of Health to The Institute for Cancer Research, and also an appropriation from the Commonwealth of Pennsylvania to The Institute for Cancer Research.

The technical assistance of Eileen Starkey, Roberta Ridley, and Mary Dolack is appreciated.

LITERATURE CITED

1. **Adams, M. H.** 1959. Bacteriophages. Interscience Publishers, New York.
2. **Asbell, M. A., and R. G. Eagon.** 1966. Role of multivalent cations in the organization, structure, and assembly of the cell wall of *Pseudomonas aeruginosa*. J. Bacteriol. 92:380–387.
3. **Bayer, M. E.** 1974. Ultrastructure and organization of the bacterial envelope. Ann. N. Y. Acad. Sci. 235:6–28.
4. **Bayer, M. E., M. Dolack, and E. Houser.** 1977. Effects of lipid phase transition on the freeze-cleaved envelope of *Escherichia coli*. J. Bacteriol. 129:1563–1573.
5. **Bayer, M. E., J. Koplow, and H. Goldfine.** 1975. Alterations in envelope structure of heptose-deficient mutants of *Escherichia coli* as revealed by freeze-etching. Proc. Natl. Acad. Sci. U.S.A. 72:5145–5149.
6. **Bayer, M. E., and C. C. Remsen.** 1970. Structure of *Escherichia coli* after freeze-etching. J. Bacteriol. 101:304–313.
7. **Cynkin, M. A., and G. Ashwell.** 1960. Estimation of 3-deoxy sugars by means of the malonaldehyde-thiobarbituric acid reaction. Nature (London) 186:155–156.
8. **DePetris, S.** 1967. Ultrastructure of the cell wall of *Escherichia coli* and chemical nature of its constituent layers. J. Ultrastruct. Res. 19:45–83.
9. **Dubois, M., K. Gilles, J. K. Hamilton, P. A. Rebers, and F. Smith.** 1951. A colorimetric method for the determination of sugars. Nature (London) 168:167.
10. **Eagon, R. G., and K. J. Carson.** 1965. Lysis of cell walls and intact cells of *Pseudomonas aeruginosa* by ethylenediaminetetraacetic acid and by lysozyme. Can. J. Microbiol. 11:193–201.
11. **Fiil, A., and D. Branton.** 1969. Changes in the plasma membrane of *Escherichia coli* during magnesium starvation. J. Bacteriol. 98:1320–1327.
12. **Forge, A., J. W. Costerton, and K. Ann Kerr.** 1973. Freeze-etching and X-ray diffraction of the isolated double-track layer from the cell wall of a gram-negative marine Pseudomonad. J. Bacteriol. 113:445–451.
13. **Gilleland, H. E. Jr., and R. G. E. Murray.** 1976. Ultrastructural study of polymyxin-resistant isolates of *Pseudomonas aeruginosa*. J. Bacteriol. 125:267–281.
14. **Gilleland, H. E., J. D. Stinnett, and R. Eagon.** 1974. Ultrastructural and chemical alteration of the cell envelope of *Pseudomonas aeruginosa*, associated with resistance to ethylenediaminetetraacetate resulting from growth in a Mg^{2+}-deficient medium. J. Bacteriol. 117:302–311.
15. **Gilleland, H. E., J. D. Stinnett, I. L. Roth, and R. G. Eagon.** 1973. Freeze-etch study of *Pseudomonas aeruginosa*: localization within the cell wall of an ethylenediaminetetraacetate-extractable component. J. Bacteriol. 113:417–432.
16. **Gray, G. W., and S. G. Wilkinson.** 1965. The action of EDTA on *Pseudomonas aeroginosa*. J. Appl. Bacteriol. 28:153–164.
17. **Gulik-Krzywicki, T.** 1975. Structural studies of the associations between biological membrane components. Biochim. Biophys. Acta 415:1–28.
18. **Heerikhuizen, H. Van, E. Kwak, E. F. J. Van Bruggen, and B. Withold.** 1975. Characterization of a low density cytoplasmic membrane subfraction isolated from *Escherichia coli*. Biochim. Biophys. Acta 413:177–191.
19. **Holt, S., J. M. Shively, and J. W. Greenwalt.** 1974. Fine structure of selected species of the genus Thiobacillus as revealed by chemical fixation and freeze-etching. Can. J. Microbiol. 20:1347–1351.
20. **Irvin, R. T., A. K. Chatterjee, K. E. Sanderson, and J. W. Costerton.** 1975. Comparison of the cell envelope structure of a lipopolysaccharide-defective (heptose-deficient) strain and a smooth strain of *Salmonella typhimurium*. J. Bacteriol. 124:930–941.
21. **Leive, L.** 1965. A non-specific increase in permeability in *Escherichia coli* produced by EDTA. Proc. Natl. Acad. Sci. U.S.A. 53:745–750.
22. **Leive, L.** 1968. Studies on the permeability change produced in coliform bacteria by EDTA. J. Biol. Chem. 243:2373–2380.
23. **Leive, L.** 1974. The barrier function of the gram-negative envelope. Ann. N. Y. Acad. Sci. 238:109–129.
24. **Leive, L., V. K. Shovlin, and S. E. Mergenhagen.** 1968. Physical, chemical, and immunological properties of lipopolysaccharide released from *Escherichia coli* by ethylenediaminetetraacetate. J. Biol. Chem. 243:6384–6391.
25. **Levy, L., and L. Leive.** 1968. An equilibrium between two fractions of lipopolysaccharide in *Escherichia coli*. Proc. Natl. Acad. Sci. U.S.A. 61:1435–1439.
26. **Morrison, D. C., and L. Leive.** 1975. Fractions of lipopolysaccharide from *Escherichia coli* 0111:B4 prepared by two extraction procedures. J. Biol. Chem. 250:2911–2919.
27. **Nanninga, N.** 1970. Ultrastructure of the cell envelope of *Escherichia coli* B after freeze-etching. J. Bacteriol. 101:297–303.
28. **Nikaido, H.** 1973. Biosynthesis and assembly of lipopolysaccharide and the outer membrane layer of gram-negative cell wall, p. 131–268. *In* L. Leive (ed.), Bacterial membranes and walls. Marcel Dekker, New York.

29. **Roberts, N. A., G. W. Gray, and S. G. Wilkinson.** 1970. The bactericidal action of ethylenediaminetetraacetic acid on *Pseudomonas aeruginosa*. Mircobios 2:189–208.
30. **Rogers, S. W., H. E. Gilleland, Jr., and R. G. Eagon.** 1969. Characterization of a protein lipopolysaccharide complex released from cell walls of *Pseudomonas aeruginosa* by ethylenediaminetetraacetic acid. Can. J. Microbiol. 15:743–748.
31. **Schlecht, S., and O. Westphal.** 1970. Untersuchungen zur Typisierung von Salmonella R-Formen. 4. Mitteilung: Typisierung von S. minnesota R-Mutanten mittels Antibiotica. Zentralbl. Bakteriol. Parasitenkd. Infektionskr. Hyg. Abt. 1 Orig. 213:356–381.
32. **Sinsheimer, R. L.** 1966. ΦX174 DNA, p. 569–576. *In* G. L. Cantoni and D. R. Davies (ed.), Procedures in nucleic acid research. Harper and Row, New York.
33. **Sleytr, U. B., M. J. Thornley, and A. M. Glauert.** 1974. Location of the fracture faces within the cell envelope of *Acinetobacter* species strain MJT/F5/5. J. Bacteriol. 118:693–707.
34. **Smit, J., Y. Kamio, and H. Nikaido.** 1975. Outer membrane of *Salmonella typhimurium*: chemical analysis and freeze-fracture studies with lipopolysaccharide mutants. J. Bacteriol. 124:942–958.
35. **Springer, E. L., and I. L. Roth.** 1973. Electron microscopy of freeze-etched preparations of *Klebsiella pneumoniae*. Arch. Microbiol. 93:277–286.
36. **Stinnett, J. D., and R. G. Eagon.** 1975. A model system for studying protein-lipopolysaccharide synthesis, assembly and insertion in the outer membrane of *Pseudomonas aeruginosa*. Can. J. Microbiol. 21:1834–1841.
37. **Swanson, J.** 1972. Studies on gonococcus infection. II. Freeze-fracture, freeze-etch studies on gonoccoci. J. Exp. Med. 136:1258–1271.
38. **Tsien, H. C., and M. L. Higgins.** 1974. Effect of temperature on the distribution of membrane particles in *Streptococcus fecalis* as seen by the freeze-fracture technique. J. Bacteriol. 118:725–734.
39. **Van Gool, A. P., and N. Nanninga.** 1973. Fracture faces in the cell envelope of *Escherichia coli*. J. Bacteriol. 108:474–481.
40. **Wu, M. C., and E. C. Heath.** 1973. Isolation and characterization of lipopolysaccharide protein from *Escherichia coli*. Proc. Natl. Acad. Sci. U.S.A. 70:2572–2576.